

ARTICLES

Generation and Decay Dynamics of Triplet Excitons in Alq3 Thin Films under High-Density Excitation Conditions

Sadayuki Watanabe, Akihiro Furube, and Ryuzi Katoh*

*National Institute of Advanced Industrial Science and Technology (AIST),
Tsukuba Central 5, 1-1-1 Higashi, Tsukuba, Ibaraki 305-8565, Japan**Received: March 23, 2006; In Final Form: June 27, 2006*

We studied the generation and decay dynamics of triplet excitons in tris-(8-hydroxyquinoline) aluminum (Alq3) thin films by using transient absorption spectroscopy. Absorption spectra of both singlet and triplet excitons in the film were identified by comparison with transient absorption spectra of the ligand molecule (8-hydroxyquinoline) itself and the excited triplet state in solution previously reported. By measuring the excitation light intensity dependence of the absorption, we found that exciton annihilation dominated under high-density excitation conditions. Annihilation rate constants were estimated to be $\gamma_{SS} = (6 \pm 3) \times 10^{-11} \text{ cm}^3 \text{ s}^{-1}$ for single excitons and $\gamma_{TT} = (4 \pm 2) \times 10^{-13} \text{ cm}^3 \text{ s}^{-1}$ for triplet excitons. From detailed analysis of the light intensity dependence of the quantum yield of triplet excitons under high-density conditions, triplet excitons were mainly generated through fission from highly excited singlet states populated by singlet–singlet exciton annihilation. We estimated that 30% of the highly excited states underwent fission.

1. Introduction

Recently, organic light-emitting diodes (OLEDs) have begun to be used as practical devices. To improve the performance of OLEDs, the operating principles of the devices have been studied in detail.^{1,2} The primary mechanism of luminescence from OLEDs is the luminescence of excitons generated by the recombination of holes and electrons injected from electrodes. Since charge carriers recombine randomly in OLEDs, singlet and triplet excitons are generated at the ratio of 1:3. For organic molecules, which are used extensively as emitting materials, luminescence from singlet excitons (fluorescence) is strong, whereas that from triplet excitons (phosphorescence) is very weak because the energy of triplet states is converted to heat efficiently. Thus, the maximum internal emission efficiency of OLEDs is 25%. Actually, singlet excitons can also decay through nonradiative processes, and therefore the quantum yield of fluorescence is smaller than unity, suggesting that the internal emission efficiency is less than 25%. Furthermore, the actual emission efficiency is also suppressed by high-density effects. Although high current density was required for bright OLEDs, the emission efficiency decreased under high current density conditions.^{3,4} A detailed analysis of this phenomenon shows that it is due to exciton–exciton³ and exciton–charge⁴ annihilations.

Tris-(8-hydroxyquinoline) aluminum (Alq3) is among the most useful of emitting materials that have been developed.^{5,6} OLEDs based on Alq3 thin films show high performance. To further improve performance, attempts to use triplet excitons in Alq3 films have been made because triplet excitons are generated by charge recombination three times as much as singlet excitons. When phosphorescent materials are used as

guest molecules in an Alq3 film, energy transfer from triplet excitons in the film to the guest molecules occurs. As a result, phosphorescence from the guest molecule can be used efficiently. In this system, the device efficiency is reduced by triplet–triplet exciton (T–T) annihilation. Namely, T–T annihilation competes with the energy transfer.^{3,7,8} Another attempt to use triplet excitons is OLEDs using delayed fluorescence (DF).⁹ By T–T annihilation, the highly excited triplet (T_n) state is generated. Subsequently, singlet excitons are generated from the T_n state and yield delayed fluorescence. It is important to note that the generation and decay processes of triplet excitons under high exciton density conditions are important processes for OLEDs.

As mentioned above, exciton dynamics under high-density conditions play an important role in highly efficient OLEDs. To study this process, photoexcitation by intense laser pulse can be used instead of measurements of the electro-luminescence of such devices under high current density conditions. Upon photoexcitation, singlet excitons are generated selectively following the selection rule of optical transitions. Under high-density excitation conditions, singlet–singlet exciton (S–S) annihilation occurs efficiently. By the collision of two singlet excitons, molecules in the ground (S_0) state and in a highly excited singlet (S_n) state are generated. The S_n state relaxes through various processes, such as internal conversion (IC), charge separation,¹⁰ and fission to two triplet excitons.¹¹ Generation and decay processes of singlet excitons can be studied through fluorescence spectroscopy. For Alq3 films, several studies on their dynamics under high excitation density conditions have been made by monitoring fluorescence.^{12–14} Triplet excitons are populated through intersystem crossing from singlet excitons. Under high density excitation conditions, fission from

* Corresponding author. E-mail: r-katoh@aist.go.jp.

a highly excited singlet state to two triplet excitons becomes possible. The emission quantum yield of triplet exciton is negligibly small, and therefore it is difficult to detect triplet excitons by luminescence spectroscopy. For Alq3, phosphorescence spectra were measured at low temperature.^{8,9,15} However, the yield is extremely low at room temperature, and therefore it is difficult to compare its properties with those of OLED devices. To observe these nonluminescent species, transient absorption is useful. Recently, transient absorption of Alq3 molecules in solution was reported, and the spectrum due to triplet excitons was identified at around 500 nm.¹⁵

Here we study the generation and decay dynamics of triplet excitons in Alq3 thin films under high exciton density conditions through transient absorption spectroscopy. We have successfully identified the absorption spectrum of triplet excitons in Alq3 thin films and estimated the rate constants of their annihilation processes. We found that triplet excitons are generated efficiently through fission of highly excited singlet states populated by S–S annihilations under high exciton density conditions.

2. Experimental Section

Tris-(8-hydroxyquinoline) aluminum (Alq3; Dojindo, sublimated) and sodium hydroxide (Wako, GR-grade) were used without further purification. 8-Hydroxyquinolinol (8-HQ; Tokyo Kasei, GR-grade) was used after purification by recrystallization with ethanol. Distilled water (Nakalai, GR-grade), ethanol (Wako, GR-grade), and toluene (Nakalai, GR-grade) were used as solvents without further purification. Alq3 thin films were prepared by vacuum evaporation on a quartz glass substrate. The sample specimen was kept in a glass vessel filled with nitrogen gas during the measurements to avoid the influence of oxygen and water. The thickness of the sample specimens was evaluated from atomic force microscope (AFM) images and it was 100–500 nm. Structure of the film was amorphous judged by the fluorescence spectrum.¹⁶

For the nanosecond transient absorption measurements, a Nd³⁺:YAG laser (Spectra Physics, Pro-230-10) operating at 355 nm was used as the pumping light source. The pulse duration of the laser was about 8 ns. A Xe flash lamp (Hamamatsu, L4642, 2 μ s pulse duration) was used as the probing light source and irradiated the sample coaxial to the pumping laser. The probing light through the sample specimen was directed to a monochromator (Ritsu, MC-10). The intensity of the probing light was detected by a Si photodiode (Hamamatsu, S-1722) and by an InGaAs photodiode (Hamamatsu, G3476–05) for the wavelength range of 400–1000 nm and 900–1600 nm, respectively. Signals from the photodetector were processed with a digital oscilloscope (Tektronix, TDS680C) and were analyzed with a computer.

Small absorption changes at low excitation intensity were measured by a highly sensitive transient absorption spectrometer based on a system previously reported.¹⁷ This system can detect an absorbance change of 10^{-6} . The time resolution of this system was about 50 ns. Although in the reported system a Xe lamp was used as the probing light, a blue diode laser (437 nm, Neoark, TC20-4420-4.5, 20 mW) was used in the present study. The probing light was passed through the sample specimen three times to lengthen the optical path.

During the transient absorption measurements, the fluorescence intensity also was measured under the same excitation conditions. The fluorescence was directed to a monochromator through an optical fiber. Signals were detected with a photomultiplier (Hamamatsu, R928) and were processed with a digital oscilloscope (Tektronix, TDS380).

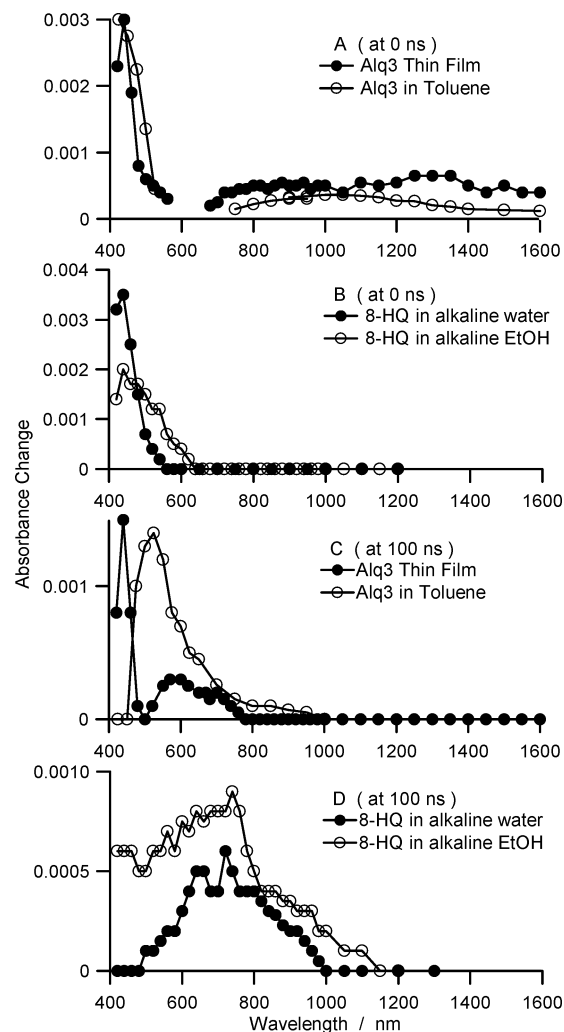


Figure 1. Transient absorption spectra just after excitation with 355-nm light. (A) Alq3 thin film and in toluene solution. (B) 8-HQ in alkaline aqueous and ethanol solutions) and 100 ns after excitation. (C) Alq3 thin film and in toluene solution. (D) 8-HQ in alkaline aqueous and ethanol solutions.

3. Results and Discussion

3.1. Assignment of Transient Absorption Spectra. Figure 1A shows the transient absorption spectrum of Alq3 in a toluene solution just after excitation (open circles), which has already been reported.¹⁸ By comparing its lifetime with fluorescence lifetime, we conclude that the spectrum is due to singlet excited state. Figure 1A also shows the transient absorption spectrum of an Alq3 thin film just after excitation with 355-nm light (closed circles). A sharp absorption band was clearly observed below 500 nm, and a broad absorption band was observed in the near-IR wavelength range. From the similarity of these spectra, the spectra of Alq3 thin films can be assigned to be due to singlet excitons.

To understand the origin of the absorption spectrum due to singlet excitons in Alq3 films, the transient absorption measurement of 8-HQ, which is a ligand molecule of Alq3, was examined in alkaline solutions of water and ethanol. The spectra just after excitation are shown in Figure 1B. In an alkaline solution, a proton is dissociated from the hydroxyl group of 8-HQ, and therefore the molecule can be considered to be in the same electronic state as the ligand in the Alq3 molecule. The absorption due to the excited singlet state of 8-HQ in solution was clearly seen below 500 nm, and no absorption was detected in the near-IR wavelength range. This indicates that

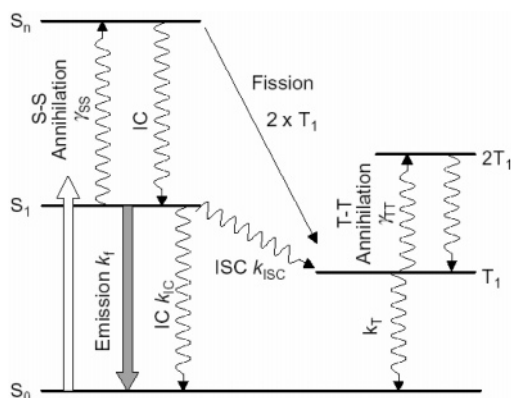


Figure 2. Generation and decay dynamics of excitons in Alq3 thin film.

the absorption band of Alq3 below 500 nm is due to the locally excited state of 8-HQ itself and that in the near-IR range it may be due to the charge-transfer transition between the center metal (Al) and the ligand.

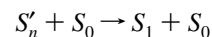
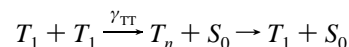
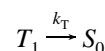
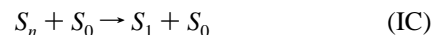
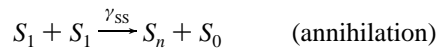
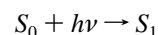
Figure 1C shows the transient absorption spectrum of an Alq3 thin film at 100 ns after excitation (closed circles). In this time range, short-lived species, singlet excited molecules disappear and long-lived species, triplet excited molecules are expected to be observed. Two absorption bands (at 450 and 600 nm) were observed. Transient absorption of Alq3 in toluene at 100 ns after excitation also was examined (open circles).¹⁸ This result is in good agreement with the spectrum previously reported by Burrows et al.¹⁵ It is obvious that two spectra of Figure 1C differ from each other. At the present excitation intensity (2.7×10^{22} photons $\text{cm}^{-2} \text{s}^{-1}$), the absorbance change is proportional to the light intensity, and therefore nonlinear optical effects, such as multiphoton ionization, can be excluded. Actually, the absorption spectra of the film is not similar to those spectra due to the anions and cations of Alq3 molecules.¹⁹ This suggests that the spectral shape of the absorption due to the excited triplet state is sensitive to the surrounding environment.

To confirm the idea above, absorption spectra due to the excited triplet state of 8-HQ in alkaline solutions of water and ethanol were examined (Figure 1D). In both solutions, an absorption peak is seen at around 700 nm, which is slightly red-shifted from that of the Alq3 solution. In the shorter wavelength range, the absorbance in the ethanol solution is negligibly small, whereas it is clearly seen in the aqueous solution. This indicates that the absorption bands due to the excited triplet state of 8-HQ are sensitive to the surrounding environment, possibly polarity of solvents. It appears that the absorption spectrum due to the triplet state consists of two absorption bands and that the absorption band in the shorter wavelength range is easily affected by the surrounding environment. Hence, the difference between the absorption spectra between in the solution and in the film can be considered to be the superposition of the two absorption bands. Apparently, the two spectra strongly overlap with each other in the solution, whereas for the thin film, on the other hand, the absorption band in the shorter wavelength range is blue-shifted. One of the possible origins of this environmental effect is a permanent dipole moment of the Alq3 molecule.²⁰

Spectral features of transient absorption in OLED materials would be important to realize for high-performance devices. It has been pointed out that the spectral position of the absorption due to excited states affects the luminescence properties of thin films under high-density excitation conditions because of nonlinear (transient) absorption effects. A decrease of the apparent

luminescence efficiency resulting from the reabsorption of transient species was reported in perylene and pyrene crystals under high exciton density conditions.²¹ A similar effect has also been pointed out for the inhabitation of the stimulated emission efficiency of dye lasers.²² This effect would be important in OLED devices operating under high current density conditions. The emission spectrum of Alq3 thin films was reported to occur at 520 nm.²³ In this wavelength range, the absorption spectra due to singlet and triplet excitons were weak (Figure 1). This would be one of the reasons for the excellent performance of OLED devices based on Alq3.

3.2. Generation and Decay Dynamics of Excitons. The generation and decay processes of excitons in an Alq3 thin film produced by photoexcitation under high-density excitation conditions is summarized based on those in organic crystals (Figure 2). It is notable that annihilation and fission processes are included, which are not important for isolated molecules in solution. Each process is described below.



In this scheme, S_0 denotes a molecule in the ground state. Upon photoexcitation, the lowest excited singlet (S_1) states are populated primarily. Then they relax to the ground state radiatively and nonradiatively. The rate constants of k_f , k_{IC} , and k_{ISC} are for fluorescence, internal conversion (IC), and intersystem crossing (ISC), respectively. Fluorescence lifetime (τ_S) is represented as $\tau_S = 1/(k_f + k_{IC} + k_{ISC})$. Singlet-singlet (S-S) annihilation also occurs with a rate constant of γ_{SS} and, subsequently, the S_0 and highly excited singlet (S_n) states are generated. The S_n state relaxes immediately through various processes, such as IC and fission to two triplet excitons. The lowest excited triplet (T_1) states are generated by ISC from S_1 states and by fission from S_n states. They relax through ISC to the ground state nonradiatively and by annihilation between triplet excitons. k_T is the ISC rate constant of triplet excitons and γ_{TT} is the annihilation rate constant of triplet excitons. Actually, radiative decay to the ground state from the T_1 state is a very slow process and therefore phosphorescence becomes negligibly weak. After annihilation of two triplet excitons, a highly excited triplet (T_n) state is populated. Some fraction forms S_n state and then fluorescence from S_1 state can be seen (delayed fluorescence).

The generation and decay processes of the S_1 state can be expressed by the following rate equation for the concentration of excitons:

$$\frac{d[S_1]}{dt} = \alpha I_{\text{ex}} - \frac{[S_1]}{\tau_s} - \frac{\gamma_{\text{SS}}}{2}[S_1]^2 \quad (1)$$

where α is the absorption coefficient for ground-state absorption, and I_{ex} is the excitation light intensity. The first term of the right-hand side of this equation is the generation term, and the second and third terms represent the relaxation due to monomolecular and annihilation processes, respectively. In case that the pulse duration of a laser is much longer than the lifetime of singlet excitons, the steady-state condition ($d[S_1]/dt = 0$) is fulfilled. Although, as will be discussed later, steady state approximation is not sufficiently fulfilled in the present experiments, we will show the solution of eq 1 under steady-state conditions to figure out excitation intensity dependence. Under low exciton density conditions, the annihilation process can be neglected. Under these conditions, eq 1 can be solved as

$$[S_1] = \alpha I_{\text{ex}} \tau_s \quad (2)$$

This clearly shows that $[S_1]$ is proportional to I_{ex} . Under high-density exciton conditions, since relaxation processes are dominated by the annihilation, the second term of the right-hand side in eq 1 becomes unimportant. Thus, eq 1 can be solved as

$$[S_1] = (2\alpha I_{\text{ex}}/\gamma_{\text{SS}})^{1/2} \quad (3)$$

so it is clear that $[S_1]$ is proportional to $I_{\text{ex}}^{1/2}$.

Next we consider the generation and decay of T_1 states. T_1 states are generated from S_1 states through the monomolecular ISC process, which is a well-known process in the relaxation dynamics of excited isolated molecules. Under high exciton density conditions in a crystalline solid, T_1 states also are generated through fission from higher excited S_n states generated by S-S annihilation. This process has been observed in anthracene.¹¹ Thus, the generation and decay kinetics of T_1 states can be described by

$$\frac{d[T_1]}{dt} = k_{\text{ISC}}[S_1] + \Phi_{\text{fission}}\gamma_{\text{SS}}[S_1]^2 - k_{\text{T}}[T_1] - \frac{\gamma_{\text{TT}}}{2}[T_1]^2 \quad (4)$$

The first and second terms on the right-hand side of eq 4 represent generation through ISC and fission, respectively. Relaxation through ISC to the ground state and T-T annihilation are expressed as the third and the fourth terms, respectively. Φ_{fission} in the second term is the efficiency of the fission process, that is, the yield of T_1 states generated from S_n states.

Under low exciton density conditions, S-S annihilation (and also fission) can be neglected. Generally, T-T annihilation is less efficient than S-S annihilation so that T-T annihilation can be neglected. Hence, from eq 2 and the first term of the right-hand side in eq 4, the initial concentration of T_1 states ($[T_1]_0$) is given by

$$[T_1]_0 = k_{\text{ISC}}\tau_s\tau_p\alpha I_{\text{ex}} \quad (5)$$

where τ_p is the laser pulse duration. It is clear that $[T_1]_0$ is proportion to I_{ex} . These dynamics generally are observed for the excited dynamics in solutions that have only a monomolecular triplet generation process. On the other hand, under high exciton density conditions in crystalline films, S-S and T-T annihilation processes have to be considered. If triplet exciton generation by fission is not efficient ($\Phi_{\text{fission}} \sim 0$) under high exciton density conditions, T_1 states are generated only by ISC from the S_1 states (ISC process). Thus, from eq 3 and

the first term of the right-hand side in eq 4, $[T_1]_0$ can be expressed by

$$[T_1]_0 = \sqrt{2}k_{\text{ISC}}\tau_p\alpha^{1/2}\gamma_{\text{SS}}^{-1/2}I_{\text{ex}}^{1/2} \quad (6)$$

In this case, $[T_1]_0$ is proportional to $I_{\text{ex}}^{1/2}$. If the fission process dominates triplet generation (fission process), $[T_1]_0$ can be obtained from eq 3 and the second term of the right-hand side in eq 4 by

$$[T_1]_0 = 2\Phi_{\text{fission}}\alpha\tau_s I_{\text{ex}} \quad (7)$$

In this case, $[T_1]_0$ is proportional to I_{ex} . It is obvious that the triplet generation process can be elucidated from the light intensity dependence of the yield of the T_1 state.

The decay kinetics of the T_1 state are described by

$$\frac{d[T_1]}{dt} = -k_{\text{T}}[T_1] - \frac{\gamma_{\text{TT}}}{2}[T_1]^2 \quad (8)$$

Under low exciton density conditions, T-T annihilation can be neglected and thus the decay profile of the T_1 state is exponential with a time constant of k_{T} . Under high exciton density conditions, the relaxation process is dominated by T-T annihilation, so the first term on the right-hand side of eq 8 can be negligible. Thus, $[T_1]$ is expressed by

$$\frac{1}{[T_1]} = \frac{\gamma_{\text{TT}}}{2}t + \frac{1}{[T_1]_0} \quad (9)$$

If eq 9 is followed, T_1 decays through bimolecular kinetics.

3.3. Annihilation Processes of Singlet Excitons. Singlet excitons emit fluorescence and therefore the density can be evaluated through fluorescence spectroscopy. The lifetime of S_1 states of Alq3 films studied was determined to be $\tau_s = 12 \pm 1$ ns, which is similar to reported values.^{1,6,14,23} The density of S_1 states in an Alq3 thin film can be estimated based on the rate equation (eq 1). The lifetime τ_s (12 ns) is slightly longer than the pulse duration τ_p of excitation light (8 ns), and therefore steady state condition is not sufficiently fulfilled under low-density excitation condition. Thus, the density could be estimated by solving eq 1 numerically after eliminating the third term of the right-hand side using the values of absorption coefficient α , τ_p , and τ_s . Absorption coefficient for ground-state absorption was estimated to be $\alpha = 1.5 \times 10^4 \text{ cm}^{-1}$ from the absorption spectra and film thickness. The closed circles in Figure 3 show the density of S_1 states in an Alq3 thin film. Under weak laser intensity conditions, the density of S_1 states is proportional to I_{ex} (upper dotted line).

At higher excitation intensity, the decay of S_1 states becomes much faster because of S-S annihilation process, suggesting that the density of the S_1 states can be evaluated under steady-state conditions. As shown in Figure 3, the density of S_1 states deviates from a linear relation and gradually approaches the line of $I_{\text{ex}}^{1/2}$ dependence (upper broken line). This is consistent with the analysis described in eq 3, namely that S-S annihilation becomes dominant, when I_{ex} becomes large. Thus, the S-S annihilation rate constant γ_{SS} is estimated to be $(6 \pm 3) \times 10^{-11} \text{ cm}^3 \text{ s}^{-1}$. The thin line in Figure 3 indicates simulated line of the density of S_1 states determined from eq 1.

The S-S annihilation rate constant γ_{SS} has been reported to be $\gamma_{\text{SS}} = (1.1 \pm 0.5) \times 10^{-10} \text{ cm}^3 \text{ s}^{-1}$ by using CW laser as excitation light source¹³ and $\gamma_{\text{SS}} = (3.5 \pm 2.5) \times 10^{-11} \text{ cm}^3 \text{ s}^{-1}$ through pulsed laser excitation (25 ps pulse duration).¹⁴ The

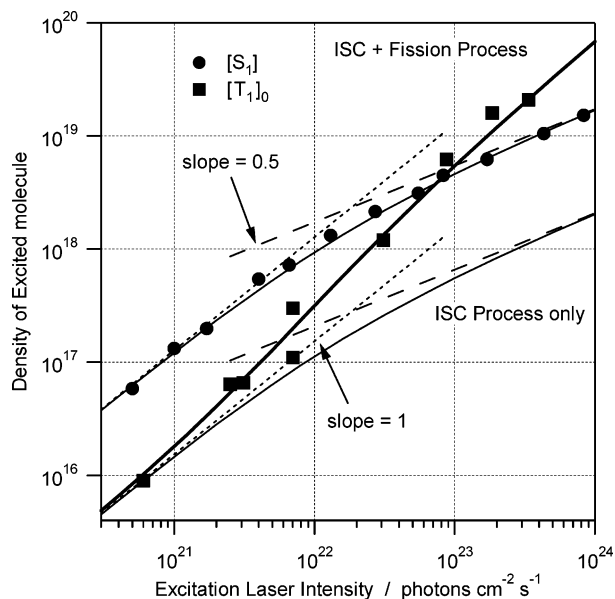


Figure 3. Excitation laser intensity dependence of the density of singlet excitons (●) and of triplet excitons (■). Simulated lines are described below. Thin line indicates $[S_1]$ determined from eq 1. Upper dotted and broken lines show the dependence expected from eqs 2 and 3, respectively. Thick line indicates $[T_1]$ determined from eq 4 substituting $\Phi_{\text{fission}} = 0.3$. Thin solid lines indicate $[T_1]$ determined from eq 4 substituting $\Phi_{\text{fission}} = 0$. Lower dotted and broken lines show the dependence expected from eqs 5 and 6, respectively.

value estimated in the present study is in good agreement with those values. It should be noted that these rate constants were similar to the value estimated by analysis of the EL efficiency under high current density conditions ($\gamma_{\text{SS}} = (5.5 \pm 0.7) \times 10^{-11} \text{ cm}^3 \text{ s}^{-1}$).²⁴ This suggests that S–S annihilation plays an important role in the OLED devices under high current density conditions.

Values of γ_{SS} have been reported for several organic crystals, and from them the motion of excitons has been discussed. For crystals having free excitons (FE), such as naphthalene and anthracene, annihilation occurs efficiently. Specifically, the values have been reported to be $1 \times 10^{-10} \text{ cm}^3 \text{ s}^{-1}$ in naphthalene and $1 \times 10^{-8} \text{ cm}^3 \text{ s}^{-1}$ in anthracene.²⁵ For crystals having self-trapped excitons (STE), such as pyrene and perylene, S–S annihilation is not efficient because of the low diffusion coefficient of STE. The rate constants of the materials have been reported to be $9 \times 10^{-15} \text{ cm}^3 \text{ s}^{-1}$ in pyrene and $8 \times 10^{-14} \text{ cm}^3 \text{ s}^{-1}$ in perylene.²⁶ The value of γ_{SS} in Alq3 thin films ($(6 \pm 3) \times 10^{-11} \text{ cm}^3 \text{ s}^{-1}$) is between the FE and STE cases. This suggests that excitons in Alq3 thin films are not in a self-trapped state and that the slowing of the exciton diffusion is due to their amorphous structure.

3.4. Annihilation Processes of Triplet Excitons. Figure 4 shows the time profile of the absorbance change of T_1 states in an Alq3 thin film excited with 355-nm light and monitored at 440 nm. The excitation light intensity was $5.5 \times 10^{22} \text{ photons cm}^{-2} \text{ s}^{-1}$, an intensity that could make high-density excitons. The lifetime of T_1 state has been reported to be $\sim 25 \mu\text{s}$ in a doped film⁷ and $56 \mu\text{s}$ in solution.¹⁵ These lifetimes are much longer than the decay of the T–T absorption shown in Figure 4, suggesting that the decay is dominated by T–T annihilation process. The reciprocal of the absorbance change as a function of time is depicted in the inset of Figure 4. The linear relation indicates a bimolecular decay process, following eq 9. Namely, the T_1 states relaxed through T–T annihilation under

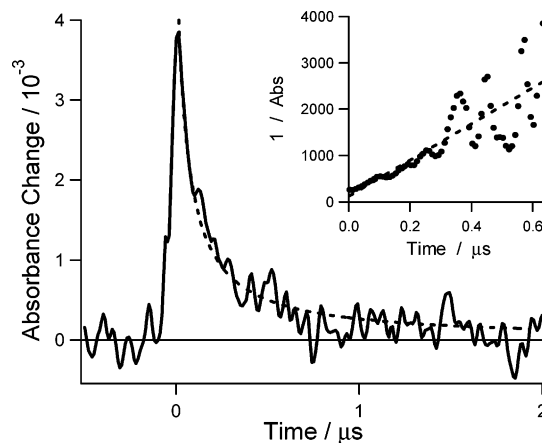


Figure 4. Time profile of absorption change of triplet excitons in an Alq3 thin film excited with 355-nm light and monitored at 440 nm. Inset shows the reciprocal plots of absorption change. Broken line indicates the curve fitted by using eq 9.

high excitation density conditions. The observed absorbance change (A) can be expressed by

$$A = \epsilon_T^{440} [T_1] d \quad (11)$$

where ϵ_T^{440} is the absorption coefficient of T_1 of Alq3 at 440 nm, and d is the sample thickness. In toluene, ϵ_T^{440} has already been estimated. It is not used as the value for Alq3 thin films because the absorption spectrum of T_1 in Alq3 thin films is different from that of Alq3 in toluene (Figure 1C). Thus, we assume that the absorption coefficient of the film at 700 nm, where the absorption band is not much affected by the environment, is the same as that in toluene ($\epsilon_T^{700} = 750 \text{ M}^{-1} \text{ cm}^{-1}$).¹⁵ Hence, ϵ_T^{440} in the film is estimated to be $4 \times 10^3 \text{ M}^{-1} \text{ cm}^{-1}$. Using the values of $\epsilon_T^{440} = 4 \times 10^3 \text{ M}^{-1} \text{ cm}^{-1}$ and $d = 400 \text{ nm}$, γ_{TT} is estimated to be $(4 \pm 2) \times 10^{-13} \text{ cm}^3 \text{ s}^{-1}$ by fitting the results with eq 9.

The annihilation process of triplet excitons in Alq3 thin films has been observed in some OLEDs. Recently, Tanaka and Tokito observed T–T annihilation process in Alq3 thin film heavily doped with tris(2-phenylpyridine)iridium [Ir(ppy)₃] at low temperature.⁸ Baldo et al.³ measured the time profiles and the excitation intensity dependence of the phosphorescence intensity from octaethynylporphine platinum (PtOET)-doped Alq3 films. They found that γ_{TT} decreases with increasing concentration of PtOET in Alq3 films, suggesting that there are interactions between host and guest excitons. By extrapolating the PtOET concentration to zero, γ_{TT} in neat Alq3 films can be estimated to be $(4 \pm 1) \times 10^{-13} \text{ cm}^3 \text{ s}^{-1}$. This is in good agreement with the value we estimate in the present study ($(4 \pm 2) \times 10^{-13} \text{ cm}^3 \text{ s}^{-1}$).

3.5. Generation Processes of Triplet Excitons. To discuss the generation processes of T_1 states in an Alq3 thin film, values of $[T_1]_0$, which are estimated by the extrapolation of the time of decay profile to zero (see Figure 4) using eq 7, are plotted as a function of excitation intensity (closed squares in Figure 3). At lower excitation intensity ($I_{\text{ex}} < 2 \times 10^{21} \text{ photons cm}^{-2} \text{ s}^{-1}$), $[T_1]_0$ can be estimated by using eq 11 and it would be proportional to I_{ex} following eq 5 (lower dotted line). From the linear relation, k_{ISC} is estimated to be $k_{\text{ISC}} = (1.0 \pm 0.5) \times 10^7 \text{ s}^{-1}$ by eq 5, taking the value of $\tau_S = 12 \text{ ns}$. As a result, the quantum yield of triplet exciton generation by ISC ($\Phi_{\text{ISC}} = k_{\text{ISC}} \tau_S$) is estimated to be $\Phi_{\text{ISC}} = 0.12 \pm 0.06$. This is significantly lower than suggested value in solution ($\Phi_{\text{ISC}} = 0.24 \pm 0.06$).¹⁵

Under high light intensity conditions ($I_{\text{ex}} > 2 \times 10^{22}$ photons $\text{cm}^{-2} \text{s}^{-1}$), $[T_1]_0$ would be proportional to $I_{\text{ex}}^{1/2}$ if the ISC process is the dominant process for triplet exciton generation (eq 6). Under this condition, the density of triplet exciton can be simulated as the thick dotted line in Figure 3. However, in reality, the concentration of triplet exciton observed (closed squares) is proportional to I_{ex} at higher intensity. This linear dependence of $[T_1]_0$ on light intensity clearly shows that the T_1 state is mainly populated through the fission process followed by eq 7.

In fact, $[T_1]_0$ is not proportional to I_{ex} in the whole intensity range in the present experiment. At lower light intensity, $[T_1]_0$ deviates from the linear relation at higher light intensity. This is because the proportionality constant of eq 5 is different from that of eq 7. From the difference, Φ_{fission} can be estimated to be 0.3 by reproducing the experimental values using eq 4 (thick line). Namely, 30% of the S_n states generated by S–S annihilation relax to two T_1 states.

Fission processes were reported in several organic crystals. For anthracene crystal, the process could be found through the magnetic field effect of prompt fluorescence under high-density excitation conditions.¹¹ In the study of picosecond transient absorption in a benzophenone crystal, it was observed that triplet exciton generation was faster than the decay of singlet exciton under high-density excitation condition. This clearly shows that triplet excitons are generated through the fission process.²⁷ Fission from the highly excited state to two triplet excitons has also been observed by VUV-photon excitation for anthracene²⁸ and perylene²⁹ crystals. It is obvious that the fission process is an important decay channel from highly excited singlet state in organic crystals.

There is a limitation from spin multiplicity on the value of Φ_{fission} in the fission process. In the fission process, the S_n state is mixed with the $2T_1$ state, which has nine different spin states. According to the theoretical model,^{30,31} six of the nine spin states have a singlet-quintet mixture character, and the remaining three spin states are purely in a triplet state. Contribution of singlet state is half of the six singlet-quintet mixture states. Thus, the maximum value of Φ_{fission} is considered to be 1/3. For Alq3 films, Φ_{fission} is estimated to be 0.3, namely all excited states having singlet character undergo triplet fission.

Recently, magnetic field effects on EL in OLEDs has been studied. Especially, for electrophosphorescence material, such as tris(2-phenyl-pyridine)iridium ($\text{Ir}(\text{ppy})_3$), a large enhancement of luminescence intensity (6%) was observed at 500 mT. The mechanism was discussed based on the Zeeman and hyperfine interactions of electron–hole pairs.³² In the present study, we found that fission from a highly excited singlet state populated by singlet exciton annihilation was the dominant generation channel for triplet exciton under high-density excitation conditions. It has been observed that fission into two triplet excitons is sensitive to an external magnetic field.^{11,28,29} Under the presence of magnetic field, the fission process is suppressed, namely, enhancement of fluorescence intensity and suppression of triplet yield can be observed. To understand magnetic field effect on EL in OLEDs, the fission process has to be taken into account.

4. Conclusion

Generation and decay dynamics of triplet excitons in Alq3 thin films was investigated. Under low excitation density conditions, triplet excitons are generated through intersystem crossing

(ISC) from singlet excitons and the quantum yield is estimated to be $\Phi_{\text{ISC}} = 0.12 \pm 0.06$. Under high excitation density conditions, annihilation and fission processes play important roles for the generation and decay dynamics. We estimated annihilation rate constants to be $\gamma_{\text{SS}} = (6 \pm 3) \times 10^{-11} \text{ cm}^3 \text{ s}^{-1}$ for single excitons and $\gamma_{\text{TT}} = (4 \pm 2) \times 10^{-13} \text{ cm}^3 \text{ s}^{-1}$ for triplet excitons. We found that under high exciton density conditions, triplet exciton generation mainly occurs through fission from highly excited singlet states generated by annihilation of two singlet excitons. We estimated that 30% of the highly excited states underwent fission. It is notable that the apparent yield of triplet excitons is proportional to the exciton concentration, whereas it decreases with increasing concentration for singlet excitons. This suggests that OLED devices that use the triplet state in Alq3 have promise for realizing high performance under high exciton concentration.

References and Notes

- Brütting, W. *Physics of Organic Semiconductors*; Wiley-VCH Verlag GmbH & Co. KGaA: Weinheim, 2005.
- Hung, L. S.; Chen, C. H. *Mater. Sci. Eng. R* **2002**, *39*, 143–222.
- Baldo, M. A.; Adachi, C.; Forrest, S. R. *Phys. Rev. B* **2000**, *62*, 10967–10977.
- Ichikawa, M.; Naitou, R.; Koyama, T.; Taniguchi, Y. *Jpn. J. Appl. Phys.* **2001**, *40*, L1068–L1071.
- Tang, C. W.; Vanslyke, S. A. *Appl. Phys. Lett.* **1987**, *51*, 913–915.
- Tang, C. W.; Vanslyke, S. A.; Chen, C. H. *J. Appl. Phys.* **1989**, *65*, 3610–3616.
- Baldo, M. A.; Forrest, S. R. *Phys. Rev. B* **2000**, *62*, 10958–10966.
- Tanaka, I.; Tokito, S. *J. Appl. Phys.* **2005**, *97*, 113532.
- Cölle, M.; Gärditz, C. *Appl. Phys. Lett.* **2004**, *84*, 3160–3162.
- Brown, C. L. *Phys. Rev. Lett.* **1968**, *21*, 215–219.
- Katoh, R.; Kotani, M. *Chem. Phys. Lett.* **1992**, *196*, 108–112.
- Garbuzov, D. Z.; Bulović, V.; Burrows, P. E.; Forrest, S. R. *Chem. Phys. Lett.* **1996**, *249*, 433–437.
- Mezyk, J.; Kalinowski, J.; Meinardi, F.; Tubino, R. *Chem. Phys. Lett.* **2004**, *395*, 321–326.
- Sokolik, I.; Priestley, R.; Walser, A. D.; Dorsinville, R.; Tang, C. W. *Appl. Phys. Lett.* **1996**, *69*, 4168–4170.
- Burrows, H. D.; Fernandes, M.; Melo, J. S.; Monkman, A. P.; Navaratnam, S. *J. Am. Chem. Soc.* **2003**, *125*, 15310–15311.
- Cölle, M.; Brütting, W. *Phys. Status Solidi* **2004**, *201*, 1095–1115.
- Yoshihara, T.; Murai, M.; Tamaki, Y.; Furube, A.; Katoh, R. *Chem. Phys. Lett.* **2004**, *394*, 161–164.
- Watanabe, S.; Murai, M.; Tamaki, Y.; Furube, A.; Katoh, R. *Proceedings of the International Symposium on Super-Functionality Organic Devices: IPAP Conf. Series 6*, 2005, pp 121–124.
- Ganzorig, C.; Fujihira, M. *Appl. Phys. Lett.* **2002**, *81*, 3137–3139.
- Curioni, A.; Boero, M.; Andreoni, W. *Chem. Phys. Lett.* **1998**, *294*, 263–271.
- Ludmer, Z.; Zeiri, L.; Starobinets, S. *Phys. Rev. Lett.* **1982**, *48*, 341–344.
- Nair, L. G. *Prog. Quantum Electron.* **1982**, *7*, 153–268.
- Kawamura, Y.; Sasabe, H.; Adachi, C. *Jpn. J. Appl. Phys.* **2004**, *43*, 7729–7730.
- Nakanotani, H.; Sasabe, H.; Adachi, C. *Appl. Phys. Lett.* **2005**, *86*, 213506.
- Pope, M.; Swenberg, C. E. *Electronic Processes in Organic Crystals and Polymers*, 2nd ed.; Oxford University Press: New York, 1999.
- Inoue, A.; Yoshihara, K.; Nagakura, S. *Bull. Chem. Soc. Jpn.* **1972**, *45*, 1973–1976.
- Katoh, R.; Kotani, M.; Hirata, Y.; Okada, T. *Chem. Phys. Lett.* **1997**, *264*, 631–635.
- Klein, G.; Voltz, R.; Schott, M. *Chem. Phys. Lett.* **1972**, *16*, 340–344.
- Takeda, Y.; Katoh, R.; Kobayashi, H.; Kotani, M. *J. Electron Spectrosc. Relat. Phenom.* **1996**, *78*, 423–426.
- Merrifield, R. E. *J. Chem. Phys.* **1968**, *48*, 4318–4319.
- Johnson, R. C.; Merrifield, R. E. *Phys. Rev. B* **1970**, *1*, 896–902.
- Kalinowski, J.; Cocchi, M.; Virgili, D.; Fattori, V.; Di Marco, P. *Phys. Rev. B* **2004**, *70*, 205303.